Random coupling of chaotic maps leads to spatiotemporal synchronization

Sudeshna Sinha[*]

Institute of Mathematical Sciences, Taramani, Chennai 600 113, India

We investigate the spatiotemporal dynamics of a network of coupled chaotic maps, with varying degrees of randomness in coupling connections. While strictly nearest neighbor coupling never allows spatiotemporal synchronization in our system, randomly rewiring some of those connections stabilizes entire networks at x^*, where x^* is the strongly unstable fixed point solution of the local chaotic map. In fact, the smallest degree of randomness in spatial connections opens up a window of stability for the synchronized fixed point in coupling parameter space. Further, the coupling ϵ_{bifr} at which the onset of spatiotemporal synchronization occurs, scales with the fraction of rewired sites p as a power law, for $0.1 < p < 1$. We also show that the regularizing effect of random connections can be understood from stability analysis of the probabilistic evolution equation for the system, and approximate analytical expressions for the range and ϵ_{bifr} are obtained.

I. INTRODUCTION

The coupled map lattice (CML) was introduced as a simple model capturing the essential features of nonlinear dynamics of extended systems [1]. Over the past decade research centered around CML has yielded suggestive conceptual models of spatiotemporal phenomena, in fields ranging from biology to engineering. In particular, this class of systems is of considerable interest in modeling phenomena as diverse as Josephson junction arrays, multimode lasers, vortex dynamics, and even evolutionary biology. The ubiquity of distributed complex systems has made the CML a focus of sustained research interest.

A very well studied coupling form in CMLs is nearest neighbor coupling. While this regular network is the chosen topology of innumerable studies, there are strong reasons to revisit this fundamental issue in the light of the fact that some degree of randomness in spatial coupling can be closer to physical reality than strict nearest neighbor scenarios. In fact, many systems of biological, technological, and physical significance are better described by randomizing some fraction of the regular links [2–7]. So here we will study the spatiotemporal dynamics of CMLs with some of its coupling connections rewired randomly, i.e., an extended system comprized of a collection of elemental dynamical units with varying degrees of randomness in its spatial connections.

Specifically, we consider a one-dimensional ring of coupled logistic maps. The sites are denoted by integers $i = 1,...,N$, where N is the linear size of the lattice. On each site is defined a continuous state variable denoted by $x_n(i)$, which corresponds to the physical variable of interest. The evolution of this lattice, under standard nearest neighbor interactions, in discrete time n is given by

$$x_{n+1}(i) = (1-\epsilon)f[x_n(i)] + \frac{\epsilon}{2}\{x_n(i+1) + x_n(i-1)\}. \tag{1}$$

The strength of coupling is given by ϵ. The local on-site map

is chosen to be the fully chaotic logistic map, $f(x) = 4x(1-x)$. This map has widespread relevance as a prototype of low dimensional chaos.

Now we will consider the above system with its coupling connections rewired randomly in varying degrees, and try to determine what dynamical properties are significantly affected by the way connections are made between elements. In our study, at every update we will connect a fraction p of randomly chosen sites in the lattice, to two other random sites, instead of their nearest neighbors as in Eq. (1). That is, we will replace a fraction p of nearest neighbor links by random connections. The case of $p=0$ corresponds to the usual nearest neighbor interaction, while $p=1$ corresponds to completely random coupling [2–7].

This scenario is much like small world networks at low p, namely, $p \sim 0.01$. Note, however, that we explore the full range of p here. In our work $0 \le p \le 1$. So the study is inclusive of, but not confined to, small world networks.

II. NUMERICAL RESULTS

We will now present numerical evidence that random rewiring has a pronounced effect on spatiotemporal synchronization. The numerical results here have been obtained by sampling a large set of random initial conditions ($\sim 10^4$), and with lattice sizes ranging from 10 to 1000.

Figures 1 and 2 display the state of the network, $x_n(i)$, $i = 1,..., N$, with respect to coupling strength ϵ, for the limiting cases of nearest neighbor interactions (i.e., $p=0$) and completely random coupling (i.e., $p=1$). It is clearly seen that the standard nearest neighbor coupling does not yield a spatiotemporal fixed point anywhere in the entire coupling range $0 \le \epsilon \le 1$ [8].

Now the effect of introducing some random connections, i.e., $p > 0$, is to *create windows in parameter space where a spatiotemporal fixed point state gains stability*, i.e., where one finds all lattice sites synchronized at $x_n(i) = x^* = 3/4$, for all sites i and at all times n. Note that $x^* = f(x^*)$ is the fixed point solution of the individual chaotic maps, and is strongly unstable in the local chaotic map. We then have for all $p > 0$, a stable region of synchronized fixed points in the parameter interval, $\epsilon_{bifr} \le \epsilon \le 1.0$. The value of ϵ_{bifr}, where the
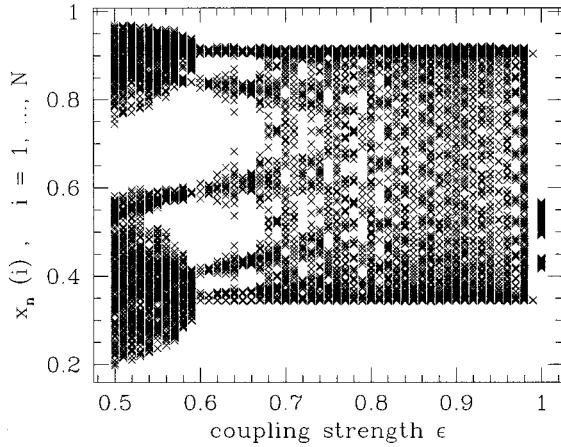
*Email address: sudeshna@imsc.ernet.in

FIG. 1. Bifurcation diagram showing values of $x_n(i)$ with respect to coupling strength ϵ, for coupled logistic maps with strictly regular nearest neighbor connections. Here the linear size of the lattice is $N=100$ and in the figure we plot $x_n(i)$ ($i=1,...,100$) over $n=1,...,5$ iterations (after a transience time of 1000) for five different initial conditions.

spatiotemporally invariant state onsets, is dependent on p. It is evident from Fig. 2 that ϵ_{bifr} for completely random coupling $p=1$ is around 0.62.

The relationship between the fraction of rewired connections p and the range, $\mathcal{R}=(1-\epsilon_{\text{bifr}})$, within which spatiotemporal homogeniety is obtained, is displayed in Fig. 3. It is clearly evident that unlike nearest neighbor coupling, random coupling leads to large parameter regimes of regular homogeneous behavior, with all lattice sites synchronized exactly at $x(i)=x^*=0.75$. Furthermore, the synchronized spatiotemporal fixed point gains stability over some finite parameter range under *any* finite p, i.e., whenever $p>0$, however small, we have $\mathcal{R}>0$. In that sense strictly nearest neighbor coupling is singular as it does not support spatiotemporal synchronization anywhere in coupling parameter
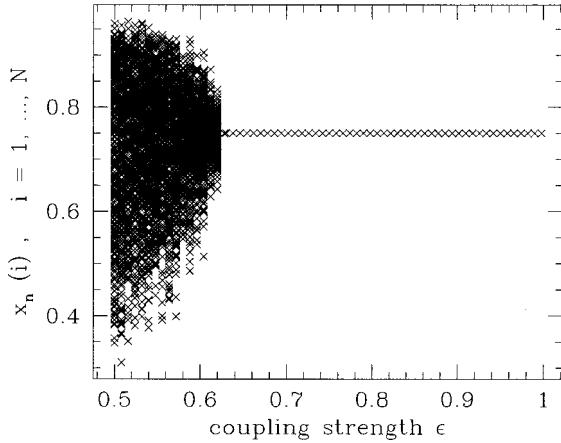

FIG. 2. Bifurcation diagram showing values of $x_n(i)$ with respect to coupling strength ϵ, for coupled logistic maps with completely random connections. Here the linear size of the lattice is $N=100$ and in the figure we plot $x_n(i)$ ($i=1,...,100$) over $n=1,...,5$ iterations (after a transience time of 1000) for five different initial conditions.
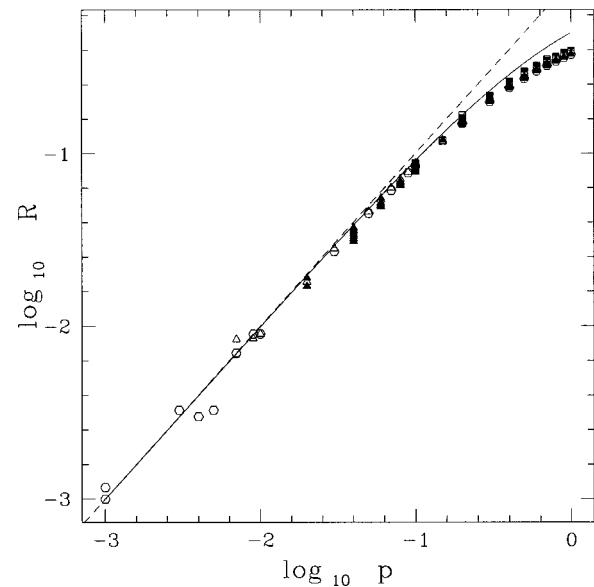

FIG. 3. The stable range R with respect to the fraction of randomly rewired sites p ($0.001 \leq p \leq 1$). The solid line displays the analytical result of Eq. (7), and the different points are obtained from numerical simulations over several different initial conditions, for four different lattice sizes, namely, $N=10$, 50, 100, and 500. The dotted line shows $\mathcal{R}=p$, and it is clear that for a large range of p the approximation holds.
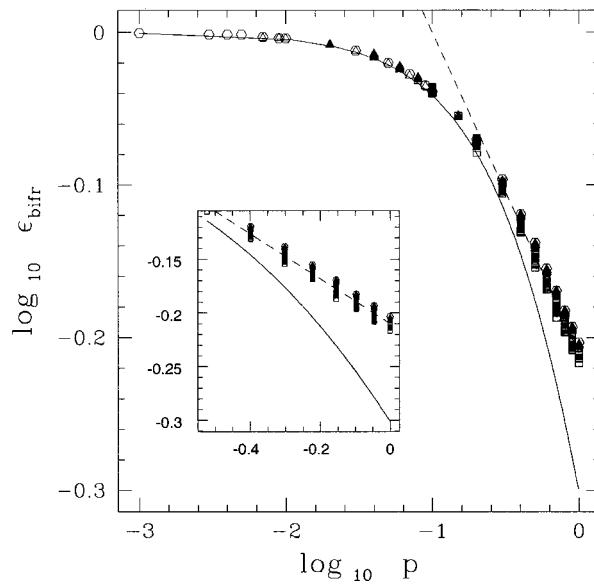

FIG. 4. The ϵ_{bifr} (i.e., the value of coupling at which the onset of spatiotemporal synchronization occurs) with respect to fraction of randomly rewired sites p ($0.001 \leq p \leq 1$). The solid line displays the analytical result of Eq. (6), and the points are obtained from numerical simulations over several different initial conditions, for four different lattice sizes, namely, $N=10$, 50, 100, and 500. The inset box shows a blow up of $0.1 < p \leq 1$. Here the numerically obtained ϵ_{bifr} deviates from the mean field results. The dashed line is the best fit straight line for the numerically obtained points in that region.

space, whereas any degree of randomness in spatial coupling connections opens up a synchronized fixed point window. Thus random connections yield spatiotemporal homogeneity here, while completely regular connections never do.

The relationship between ϵ_{bifr}, the point of onset of the spatiotemporal fixed phase, and p is shown in Fig. 4. Note that for $p < 0.1$ random rewiring does not affect ϵ_{bifr} much. Only after $p \sim 0.1$ does ϵ_{bifr} fall appreciably. Further, it is clearly evident that for $0.1 < p \leq 1$ the lower end of the stability range falls with increasing p as a well defined power law. Note that lattice size has very little effect on ϵ_{bifr}, and the numerically obtained ϵ_{bifr} for ensembles of initial random initial conditions over a range of lattice sizes $N = 10, 50, 100$, and 500 fall quite indistinguishably around each other.

The robust spatiotemporal fixed point supported by random coupling may have significant ramifications. It has immediate relevance to the important problem of controlling/synchronizing extended chaotic systems [10,11]. Obtaining spatiotemporal synchronization by introducing some random spatial connections may have practical utility in the control of large interactive systems. The regularizing effect of random coupling may then help to devise control methods for spatially extended interactive systems, as well as suggest natural regularizing mechanisms in physical and biological systems.

III. ANALYTICAL RESULTS

We shall now analyze this system to account for the much enhanced stability of the homogeneous phase under random connections. The only possible solution for a spatiotemporally synchronized state here is one where all $x_n(i) = x^*$, and $x^* = f(x^*)$ is the fixed point solution of the local map. For the case of the logistic map $x^* = 4x^*(1 - x^*) = 3/4$.

To calculate the stability of the lattice with all sites at x^* we will construct an *average probabilistic evolution rule* for the sites, which becomes a sort of *mean field version of the dynamics*. Some effects due to fluctuations are lost, but as a first approximation we have found this approach qualitatively right, and quantitatively close to the numerical results as well.

We take into account the following: all sites have probability p of being coupled to random sites, and probability $(1 - p)$ of being wired to nearest neighbors. Then the averaged evolution equation of a site j is

$$x_{n+1}(j) = (1 - \epsilon)f[x_n(j)] + (1 - p)\frac{\epsilon}{2}\{x_n(j+1) + x_n(j-1)\}$$

$$+ p\frac{\epsilon}{2}\{x_n(\xi) + x_n(\eta)\}, \tag{2}$$

where ξ and η are random integers between 1 and N.

To calculate the stability of the coherent state, we perform the usual linearization. Replacing $x_n(j) = x^* + h_n(j)$, and expanding to first order gives

$$h_{n+1}(j) = (1 - \epsilon)f'(x^*)h_n(j) + (1 - p)\frac{\epsilon}{2}\{h_n(j+1)$$

$$+ h_n(j-1)\} + p\frac{\epsilon}{2}\{h_n(\xi) + h_n(\eta)\}$$

$$\approx (1 - \epsilon)f'(x^*)h_n(j) + (1 - p)\frac{\epsilon}{2}\{h_n(j+1)$$

$$+ h_n(j-1)\}, \tag{3}$$

as to a first approximation one can consider the sum over the fluctuations of the random neighbors to be zero. This approximation is clearly more valid for small p.

For stability considerations one can diagonalize the above expression using a Fourier transform $[h_n(j) = \Sigma_q \phi_n(q)\exp(ijq)$, where q is the wave number and j is the site index], which finally leads us to the following growth equation:

$$\frac{\phi_{n+1}}{\phi_n} = f'(x^*)(1 - \epsilon) + \epsilon(1 - p)\cos q, \tag{4}$$

with q going from 0 to π. Clearly the stabilization condition will depend on the nature of the local map $f(x)$ through the term $f'(x)$ in Eq. (4). Considering the fully chaotic logistic map with $f'(x^*) = -2$, one finds that the growth coefficient that appears in this formula is smaller than one in magnitude if and only if

$$\frac{1}{1+p} < \epsilon < 1, \tag{5}$$

i.e.,

$$e_{\mathrm{bifr}} = \frac{1}{1+p} \tag{6}$$

and the range of stability $\mathcal{R}$ is

$$\mathcal{R} = 1 - \frac{1}{1+p} = \frac{p}{1+p}. \tag{7}$$

For small p ($p \ll 1$) standard expansion gives

$$\mathcal{R} \sim p. \tag{8}$$

The usual case of regular nearest neighbor couplings, $p = 0$, gives a null range, as the upper and lower limits of the range coincide. When all connections are random, i.e., $p = 1$ the largest stable range is obtained, and the lower end of the stable window ϵ_{bifr} is minimum, with $\epsilon_{\mathrm{bifr}} = 1/2$. So stability analysis also clearly dictates that enhanced stability of the homogeneous phase must occur under random connections, just as numerical evidence shows.

Figure 3 exhibits both the analytical expression of Eq. (7) and the numerically obtained points for comparison. It is clear that for small p the numerically obtained $\mathcal{R} \sim p$ is in complete agreement with the analytical formula. But for higher p some deviation is discernable, as the ignored effect of the fluctuating contributions from random neighbors is

weighted by p, and hence more pronounced for large p. Here the numerically obtained result goes as

$$\epsilon_{\mathrm{bifr}} \sim p^{-\phi}, \qquad (9)$$

for $0.1 < p \leq 1$, with $\phi \sim 0.2$ (see Figs. 4 and 7).

Note that when $p < 0.1$ the effect on ϵ_{bifr} is not significant. Only when $0.1 < p \leq 1$ does ϵ_{bifr} fall appreciably. So connecting elements in a small world network is not sufficient to make much difference to the onset of the stable spatiotemporally synchronized state [9].

IV. RESULTS FROM OTHER MODELS

In order to examine the range of applicability of this phenomena we have examined coupled tent maps and coupled sine circle maps as well. In the case of coupled tent maps the local map in Eq. (1) is given as

$$f(x) = 1 - 2|x - 1/2|. \qquad (10)$$

The tent map has an unstable fixed point at $x^* = 2/3$, with local slope $f'(x^*) = -2$. For coupled circle map networks the local map in Eq. (1) is given as

$$f = x + \Omega - \frac{K}{2\pi}\sin(2\pi x) \qquad (11)$$

and Eq. 1 is taken mod 1. In the representative example chosen here the parameters of the circle map are $\Omega = 0$, $K = 3$. Here too the local map has a strongly unstable fixed point at $x^* = (1/2\pi)\sin^{-1}(\Omega/K)$, with $f'(x^*) = -2$. Numerics very clearly show that both these systems yield the same phenomena as logistic maps, namely, one obtains a stable range for spatiotemporal synchronization on random rewiring (see Figs. 5 and 6 for the limiting cases of $p = 0$ and $p = 1$ in coupled circle maps).

Since the $f'(x^*)$ of both the tent map and the circle map above is -2, we expect from our analysis [Eq. (4)] that their ϵ_{bifr} and $\mathcal{R}$ will be the same as for logistic maps. This is indeed exactly true, as is evident from Fig. 7 that displays the point of onset of spatiotemporal synchronization for all three cases. In fact, the numerically obtained ϵ_{bifr} values for ensembles of coupled tent, circle, and logistic maps fall indistinguishably around each other, even for high p where Eq. (4) is expected to be less accurate.

Additionally, one can infer from the stability analysis above, how strongly unstable the local maps can possibly be while still allowing random connections to stabilize the spatiotemporal fixed point. From Eq. (4) it follows that the onset of spatiotemporal regularity is governed by the condition

$$|f'(x^*)| < \frac{1 - \epsilon + \epsilon p}{1 - \epsilon} = 1 + \frac{\epsilon p}{1 - \epsilon}. \qquad (12)$$

Clearly then, locally unstable maps with $|f'(x^*)| > 1$ can be stabilized by any finite p, i.e., by any degree of randomness in the coupling connections. As coupling strength ϵ and fraction of rewiring p increases, maps with increasingly unstable fixed points can be synchronized stably by random rewiring. For regular coupling ($p = 0$) on the other hand the local in-
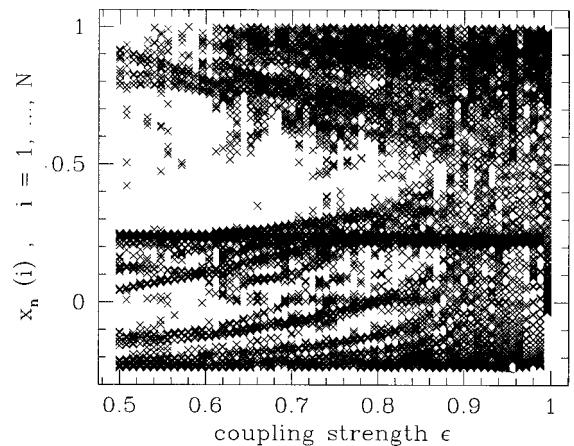

FIG. 5. Bifurcation diagram showing values of $x_n(i)$ with respect to coupling strength ϵ, for coupled sine circle maps with strictly regular nearest neighbor connections. Here the linear size of the lattice is $N = 100$ and in the figure we plot $x_n(i)$ ($i = 1,...,100$) over $n = 1,...,5$ iterations (after a transience time of 1000) for five different initial conditions.

stability can only be as large as 1, i.e., if and only if the local components possess stable fixed points can their network be stabilized at spatiotemporal fixed points, as numerics have already shown.

Lastly, in certain contexts, especially neuronal scenarios, the randomness in coupling may be *static*. In the presence of such quenched randomness in the couplings, once again one obtains a stable range $\mathcal{R}$ for spatiotemporal synchronization. But unlike dynamical rewiring, where the $\mathcal{R}$ is independent of the size and initial preparation of the lattice and its connections, here there is a spread in the values of $\mathcal{R}$ obtained from different (static) realizations of the random connections. Furthermore, this distribution of $\mathcal{R}$ is dependent on the size of network. For instance, on an average, networks of size $N = 10$ with fully random static connections ($p = 1$) yield $\epsilon_{\mathrm{bifr}} \sim 0.75$ and those of size $N = 100$ yield $\epsilon_{\mathrm{bifr}} \sim 0.85$,
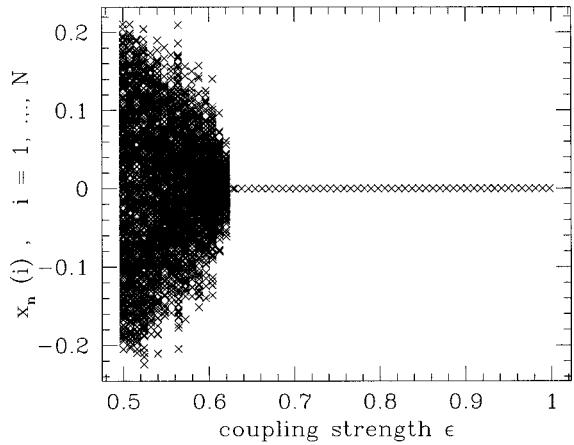

FIG. 6. Bifurcation diagram showing values of $x_n(i)$ with respect to coupling strength ϵ, for coupled sine circle maps with completely random connections. Here the linear size of the lattice is $N = 100$ and in the figure we plot $x_n(i)$ ($i = 1,...,100$) over $n = 1,...,5$ iterations (after a transience time of 1000) for five different initial conditions.
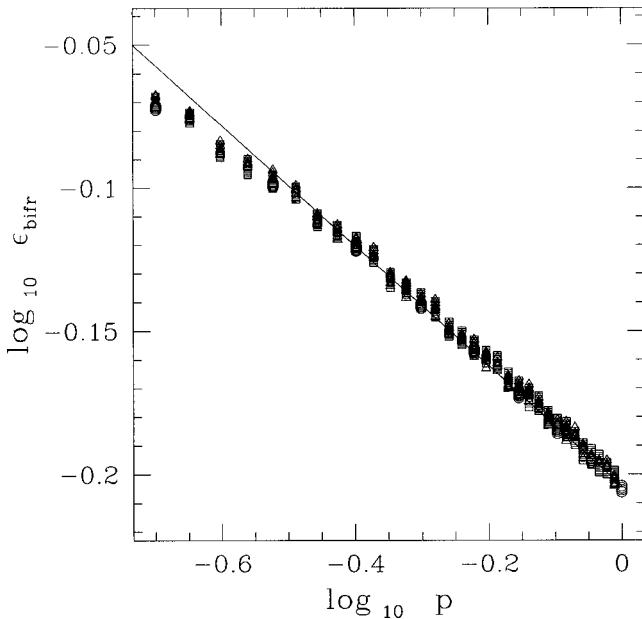
FIG. 7. Plot of ϵ_{bifr} (i.e., the value of coupling at which the onset of spatiotemporal synchronization occurs) with respect to fraction of randomly rewired sites p ($0.2 \leqslant p \leqslant 1$). The points are obtained from numerical simulations over several different initial conditions, for lattice size $N = 50$, for the case of coupled tent maps (open squares), coupled circle maps (open triangles), and coupled logistic maps (open circles). The solid line displays the best fit straight line for the numerically obtained points.
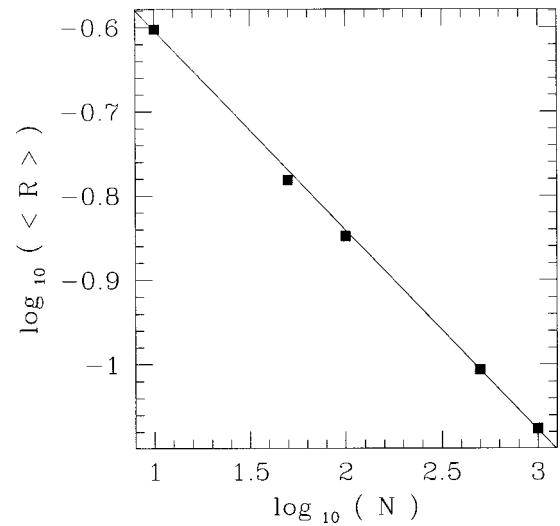

FIG. 8. Plot of the average stable range $\langle \mathcal{R} \rangle$ of spatiotemporal synchronization obtained in the case of static random connections with respect to network size N, for rewired fraction $p = 1$. Here we average $\mathcal{R}$ over 10^4 different realizations of static random connections. The solid line shows the best fit line to the numerically obtained data, indicating clear scaling.

as opposed to $\epsilon_{\text{bifr}} \sim 0.62$ obtained for all N for dynamically updated random connections. Figure 8 displays the average range $\langle \mathcal{R} \rangle$ with respect to network size N, indicative of clear scaling behavior,

$$\langle \mathcal{R} \rangle \sim N^{-\nu}, \tag{13}$$

with $\nu \sim 0.24$. This suggests that the range narrows *slowly* with increasing network size. So, while in the limit of infinite lattices there will be no spatiotemporal synchronization, for finite networks static randomness will lead to stable windows of spatiotemporal synchronization.

This behavior can be understood by examining the linear stability of the homogeneous solution: $x_n(j) = x^*$ for all sites j at all times n. For instance, for the case of fully random static connections $p = 1$, considering the dynamics of small perturbations over the network one obtains the transfer matrix connecting the perturbation vectors at successive times to be a sum of a $N \times N$ diagonal matrix, with entries $(1 - \epsilon) f'(x^*)$, and $(\epsilon/2) \mathbf{C}$ where $\mathbf{C}$ is a $N \times N$ sparse nonsymmetric matrix with two random entries of 1 on each row. Now the minimum of the real part of the eigenvalues of $\mathbf{C}$, λ_{min}, crucially governs the stability. Typically $\epsilon_{\text{bifr}} = 2/\{\lambda_{\text{min}} + 4\}$ when $f'(x^*) = -2$. Now the values of λ_{min} obtained from different static realizations of the connectivity matrix $\mathbf{C}$ are distributed differently for different sizes N. For small N

this distribution is broad and has less negative averages (~ -1). On the other hand, for large N the distribution gets narrower and tends towards the limiting value of -2. This results in a larger range of stability, and greater spread in ϵ_{bifr} for small networks. In fact, for small N, certain static realizations yield a larger range of stability ($\mathcal{R} \sim 1/2$) than dynamic rewiring.

V. CONCLUSIONS

In summary then, we have shown that random rewiring of spatial connections has a pronounced effect on spatiotemporal synchronization. In fact, strictly nearest neighbor coupling is not generic, in that it does not support any spatiotemporal fixed point phase, while the smallest degree of random rewiring has the effect of creating a window of spatiotemporal invariance in coupling parameter space. Further, the regularizing effect of random connections can be understood from stability analysis of the probabilistic evolution equation for the system, and approximate analytical expressions for the range and onset of spatiotemporal synchronization have been obtained. The key observation that *random coupling regularizes* may then help to devise control methods for spatially extended interactive systems, as well as suggest natural regularizing mechanisms in physical and biological systems.

[1] *Theory and Applications of Coupled Map Lattices*, edited by K. Kaneko (Wiley, New York, 1993); J. Crutchfield and K. Kaneko, in *Directions in Chaos*, edited by Hao Bai-Lin (World Scientific, Singapore, 1987), and references therein.

[2] D. J. Watts and Strogatz, Nature (London) **393**, 440 (1998); J. J. Collins and C. C. Chow, *ibid.* **393**, 409 (1998).

[3] J. J. Hopfiled and A. V. M. Hertz, Proc. Natl. Acad. Sci. U.S.A. **92**, 6655 (1995).

[4] S. A. Pandit and R. E. Amritkar, Phys. Rev. E **60**, R1119 (1999); **63**, 041104 (2001).

[5] K. Christiansen *et al.*, Phys. Rev. Lett. **81**, 2380 (1998).

[6] M. Barthelemy and L. A. Nunes Amaral, Phys. Rev. Lett. **82**, 3180 (1999).

[7] F. Bagnoli and F. Cecconi, Phys. Lett. A **282**, 9 (2001).

[8] Only the strong coupling range $1/2 \leq \epsilon \leq 1$ is displayed in Figs. 1 and 2. The weak coupling range $0 \leq \epsilon \leq 1/2$ (not shown) is strongly irregular for both $p=0$ and $p=1$.

[9] The range of stability also depends on the specific coupling form. For instance, if one considered the future-coupled case, where the coupling occurs through $f(x)$, then an additional factor of $f'(x)$ multiplies the second term in Eq. (4). The va-lidity of the approximation in Eq. (3) also depends on the coupling form. Again for the future-coupled case the approximation is much worse as the term ignored is weighted by an additional factor of $f'(x)$, which is greater than 1 for chaotic maps. In fact, for the future-coupled case numerical evidence of spatial synchronization is obtained for chaotic logistic maps with $f(x) = rx(1-x)$, only when $r < 4$, e.g., around $r \sim 3.8$. But even for $r \sim 4$, where exact synchronization is not obtained, the roughness of the spatial profile is much less than that for regular nearest neighbor coupling. So the random coupling does have a regularizing effect there as well, though not as complete as in the examples in this work.

[10] W. L. Ditto *et al.*, Nature (London) **376**, 465 (1995); S. Sinha and N. Gupte, Phys. Rev. E **58**, R5221 (1998); **64**, R015203 (2001).

[11] Some references of this rapidly growing field of interest are: L. Pecora and T. M. Caroll, Phys. Rev. Lett. **64**, 821 (1990); Phys. Rev. A **44**, 2374 (1991); T. L. Caroll, Phys. Rev. E **50**, 2580 (1994); F. Heagy, T. L. Caroll, and L. M. Pecora, *ibid.* **50**, 1874 (1994); D. Auerbach, Phys. Rev. Lett. **72**, 1184 (1994).